Nonmonotonic Evolution of Density Fluctuations during Glass Relaxation

John C. Mauro,[1] Sezen Soyer Uzun,[2] Wim Bras,[3] and Sabyasachi Sen[2]
[1]*Science and Technology Division, Corning Incorporated, Corning, New York 14831, USA*
[2]*Department of Chemical Engineering and Materials Science, University of California–Davis, Davis, California 95616, USA*
[3]*Netherlands Organization for Scientific Research (NWO), DUBBLE-CRG/ESRF, B.P. 220, F-38043 Grenoble Cedex, France*

(Received 30 December 2008; published 17 April 2009)

A fundamental understanding of glass relaxation behavior is vital to the glass and polymer science communities. While prior work has focused on relaxation of first-order thermodynamic properties such as enthalpy and density, we present theoretical and experimental results showing that fluctuations in enthalpy and density relax nonmonotonically. These results provide direct evidence for dynamical heterogeneities and their close association with density fluctuations. Our results imply that density fluctuations, and hence light scattering, can be minimized through design of thermal history.

DOI: 10.1103/PhysRevLett.102.155506 PACS numbers: 61.43.Fs, 61.05.cf, 61.20.Lc

Two key phenomena that govern the physics of the glassy state are (i) the liquid-to-glass transition, wherein a kinetic constraint is imposed on a liquid to induce vitrification, and (ii) the spontaneous relaxation of a glass toward the liquid state, during which the kinetic constraint is overcome [1,2]. Whereas previous studies have focused on the relaxation of first-order properties such as enthalpy, density, or refractive index [3], here we investigate the behavior of enthalpy and density fluctuations during relaxation. Our results show that the magnitude of these fluctuations relaxes nonmonotonically as a glass anneals at constant temperature. Such behavior is direct evidence for the presence of dynamical heterogeneities governing the nonexponentiality of the relaxation function.

Our theoretical results are based on the energy landscape formalism of Stillinger and Weber [4,5]. Since all practical glasses are formed under isobaric conditions, our model is formulated in terms of an enthalpy landscape [6,7]. For an N-atom system, the enthalpy landscape is a $(3N+1)$-dimensional hypersurface containing a multitude of local minima, each corresponding to a mechanically stable configuration of atoms known as an "inherent structure." The volume of configurational phase space that drains to a particular minimum is called a "basin" [4,5]. The utility of the enthalpy landscape approach lies in the ability to separate the high frequency vibrations within a basin from the slower interbasin transitions.

For our simulations we employ the Mauro-Loucks enthalpy landscape model of selenium [8]. Selenium has a low glass transition temperature of about 318 K [9] and is well known as a fragile liquid with nonexponential decay behavior [10,11]. Following Stillinger and Weber [4,5], the Mauro-Loucks approach involves first mapping the continuous enthalpy landscape to a discrete set of inherent structures and transition points. The landscape itself is computed using two- and three-body potentials derived from quantum-level simulations [8]. A separate calculation is required to compute the inherent structure density of states [12]. The dynamics of the system can be computed using a master equation solver [13] to access long time scales. Enthalpy fluctuations are computed by

$$\sigma_H(t) = \sqrt{\sum_i p_i(t) H_i^2 - \left[\sum_i p_i(t) H_i\right]^2},$$

where $\sigma_H(t)$ is the standard deviation of enthalpy fluctuations, $p_i(t)$ is the probability of occupying basin i at time t, and H_i is the enthalpy of basin i. Density fluctuations are computed using an analogous formula for molar volume.

We model three selenium systems, each initially equilibrated at a given fictive temperature: $T_f = 327.6$ K (for glass I), $T_f = 313.0$ K (glass II), and $T_f = 290.0$ K (glass III). All systems are instantaneously quenched to 298.4 K, and we compute the relaxation behavior during an isothermal hold at this temperature. The enthalpy relaxation curves for the three systems are shown in Fig. 1(a). Since glasses I and II are both down-quenched from an initially equilibrated state, they undergo a monotonic decrease in enthalpy. Glass III, having been up-quenched from a lower fictive temperature, experiences a monotonic increase. While the monotonic relaxation in Fig. 1(a) is expected, Fig. 1(b) shows that the standard deviation of enthalpy fluctuations relaxes nonmonotonically for all three systems. In each glass the fluctuations initially overshoot the equilibrium value and then relax from the other side after passing through a stationary point.

Figure 2 plots the evolution of (a) average density and (b) density fluctuations for the three selenium glasses. Glasses I and II start at higher fictive temperatures and hence relax to higher values of density. Both of these glasses display minima in density fluctuations during relaxation, similar to the enthalpy fluctuation results shown in Fig. 1(b). Glass III experiences a maximum in density fluctuations.

This nonmonotonic relaxation behavior of density fluctuations is confirmed experimentally for a multicomponent oxide network glass, Corning code 7059. This glass has a calorimetric glass transition temperature of about

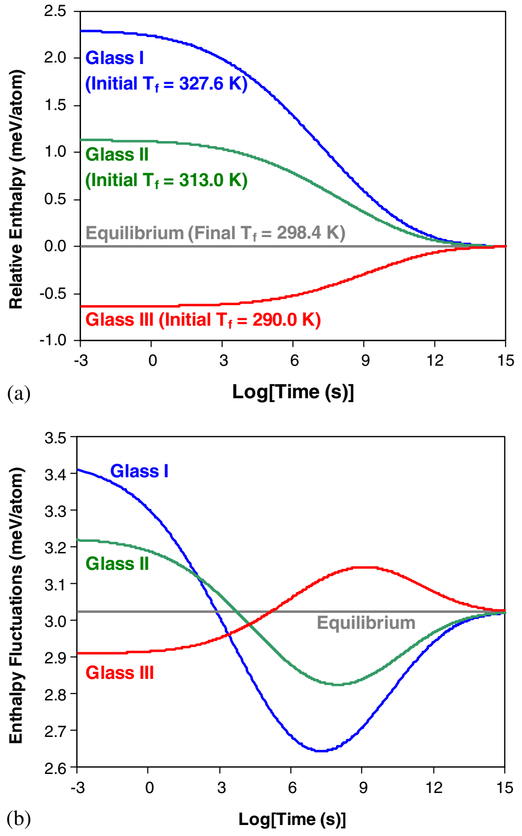

FIG. 1 (color online). Isothermal relaxation of selenium glass at 298.4 K after prior equilibration at three different fictive temperatures. (a) Computed relaxation of average enthalpy with respect to the final equilibrated system. (b) Evolution of enthalpy fluctuations as the three glasses relax toward equilibrium.

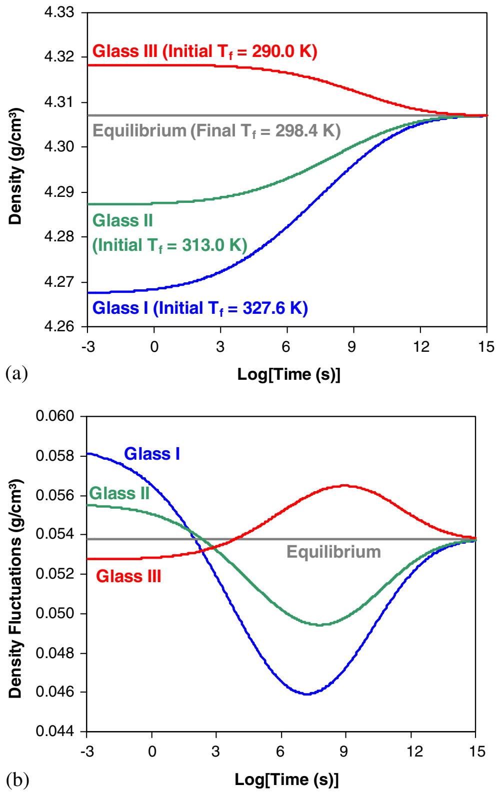

FIG. 2 (color online). Computed evolution of (a) average density and (b) density fluctuations for the three selenium glasses from Fig. 1.

925 K [14], and a composition (mol %) of 12.5% BaO, 8.5% Al_2O_3, 16% B_2O_3, and 63% SiO_2. Drawn sheets of this glass (1.1 mm thick) were obtained from Corning Inc. and annealed at 955 K for 4 h followed by rapid quenching in flowing air to ensure identical starting fictive temperature. Density measurements indicated the T_f to be ~953 K [15]. Subsequently, 10 mm × 10 mm plates with 100 μm thickness were cut and polished for *in situ* small-angle x-ray scattering (SAXS) measurements of the temporal evolution of density fluctuation at 868 K. These measurements were performed at beam line 7.3.3 at the Advanced Light Source synchrotron radiation facility at Lawrence Berkeley Laboratory. Polished glass plates were heated on a commercial hot stage (THMS600, Linkam Scientific Instruments Ltd.). Temperature control was achieved through the use of a TMS94 temperature programmer connected to the stage. This setup provided an available wave vector q range of 0.01–0.5 $Å^{-1}$. An incident energy of 10 keV was used; scattered radiation was detected using a CCD camera and integrated radially to obtain the scattered intensity $I(q)$ as a function of q. The $I(q)$ vs q data were collected for 300 s at room temperature, corresponding to $T_f = 953$ K. Subsequently, the sample was heated to 868 K at a rate of 40 K/min and equilibrated at this temperature for over a period of 20 h once the target temperature was reached. The scattering data were collected at different time steps for 300 s during this period of equilibration to monitor the temporal evolution of density fluctuation following the jump in T_f. Since the primary interest is in the accurate measurement of relative changes in $I(q)$ with time, no attempt has been made to obtain the absolute values of scattered intensities. It has been shown in previous studies that $I(q)$ in the low-q limit is directly proportional to the amplitude of the density fluctuation in a material and can be obtained by linearly extrapolating $\log I(q)$ vs q^2 data down to $q = 0$ [16–18]. We have followed a similar procedure although the relative variation in $I(q)$ with annealing time has been found to remain independent of q at least up to $q = 0.5$ $Å^{-1}$ corresponding to real space distances of ~1.2 nm, within the limits of experimental error. This result is consistent with the characteristic length scale of density fluctuations in glasses, which is expected to be of the order of a few nanometers [18,19]. The relative variation in density fluctuation thus obtained is shown in Fig. 3 as a function of annealing time at 868 K.

It may be noted that for a multicomponent glass such as 7059, the $I(q)$ at low q is a measure of both density and concentration fluctuations. However, it is well known [16,17] that concentration fluctuation is frozen at a significantly higher fictive temperature than density fluctuation.

Typically, for SAXS experiments concentration fluctuation is arrested at a fictive temperature where viscosity is $\sim 10^8$ Pa · s corresponding to at $T_g/T = 0.85$ for the 7059 glass [15,17]. Such high fictive temperature for concentration fluctuation results from the fact that it requires long-range (nanometer scale) diffusion of constituent atoms. Such diffusion would be negligible for the annealing experiment reported here that was carried out at $T_g/T \sim 1.07$ where the viscosity is simply too high ($\sim 10^{14.5}$ Pa · s for 7059 glass) for long-range diffusion. Moreover, from statistical thermodynamics, the equilibrium value of density fluctuation is expected to be linearly proportional to the nominal fictive temperature T_f. The nominal T_f in this experiment changes from 953 to 868 K while the normalized density fluctuation changes from 1 to 0.85. The ratios of the initial and final magnitudes of density fluctuation and T_f values are indeed in good agreement (within $\sim 5\%$). Therefore, the relative variation in $I(q)$ with annealing time as observed in these experiments can be safely ascribed entirely to density fluctuation.

It is clear from Fig. 3 that the density fluctuation in the 7059 glass initially decreases upon down-quenching and overshoots the equilibrium value. The density fluctuation then goes through a minimum for annealing times of ~ 8 h and subsequently starts increasing until it finally reaches equilibrium for annealing times longer than ~ 17 h. Detailed density and structural relaxation measurements under such conditions have already been reported for this glass in the literature [15]. Specifically, the density of 7059 glass was found to relax monotonically with time upon down-quenching from 953 to 868 K following a stretched exponential relaxation function [15]. This contrasting monotonic versus nonmonotonic relaxation behavior of density and its fluctuations, respectively, in 7059 glass is indeed similar to the simulation results obtained for glassy selenium, as discussed above.

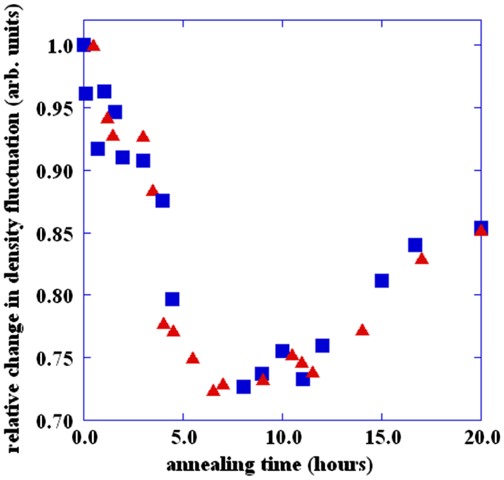

FIG. 3 (color online). Isothermal relaxation of density fluctuation of 7059 glass at 868 K after prior equilibration at 953 K. Red triangles and blue circles represent results from two separate runs.

Our experimental and modeling results provide direct evidence for the presence of dynamical heterogeneities governing the relaxation behavior in the glassy state. Figure 4 illustrates this point for selenium, showing the computed molar volume distributions of (a) the down-quenched glass I and (b) the up-quenched glass III. The relaxation of glass I involves a downward shift in the molar volume distribution (i.e., from low density to high density). The solid gray (blue) line in Fig. 4(a) shows the intermediate molar volume distribution as the glass passes through the minimum in density fluctuations (at $10^{7.4}$ s). While the lower tail of the volume distribution has not changed, the upper tail has relaxed downward toward equilibrium. In other words, the regions of the glass with higher molar volume relax faster than those regions with lower molar volume. The result is a narrowing of the volume distribution and a minimization of the density fluctuations during the relaxation process. Whereas the down-quenched glass in Fig. 4(a) displays a minimum in density fluctuations, the up-quenched glass in Fig. 4(b) experiences a maximum as the mean of the volume distribution shifts downward. The solid gray (red) line in Fig. 4(b) shows the molar volume distribution at the time of maximum fluctuations ($10^{9.3}$ s). As with the down-quenched

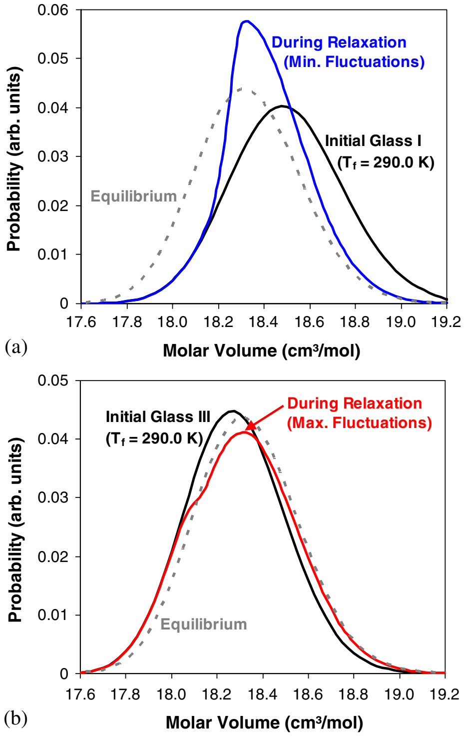

FIG. 4 (color online). Molar volume distributions of (a) glass I and (b) glass III from Fig. 2. The initial distributions are shown by the solid black lines; the equilibrated distribution is indicated by the dashed gray line in both plots. The gray solid lines show the molar volume distributions at the two critical points: (a) the minimum in fluctuations [solid gray (blue) line] for glass I at $10^{7.4}$ s and (b) the maximum in fluctuations [solid gray (red) line] for glass III at $10^{9.3}$ s.

glass, the lower tail of the distribution still traces that of the initial distribution while the upper tail has relaxed toward equilibrium. Since the mean volume shifts upward, this naturally leads to a maximum in the density fluctuations during relaxation. The higher density regions are allowed to equilibrate only at longer times. This result can be understood in terms of the number of transition states available. From the calculations of Mauro and Loucks [8], regions with lower density have a greater number of available transition points, and hence a higher entropic component lowering the free energy activation barrier.

Dynamical heterogeneities near glass transition have been observed previously in binary Lennard-Jones systems [20], colloidal suspensions [21], soft spheres [22], water [23], and organic molecular liquids [24], although how they relate to structure had been a matter of controversy [25]. Our results directly establish this connection by indicating that nanometer-scale regions of different densities in the glass relax independently and are characterized by different relaxation rates.

The results presented here imply that thermal history may be used to tailor glasses to achieve specified levels of density fluctuations, allowing increased control over properties such as light scattering and related thermodynamic properties, viz., heat capacity and thermal expansion coefficient. Our results also provide insight into the ubiquitously observed nonexponential nature of the relaxation decay function [10], as the individual relaxation modes may be associated with different nanometric spatial regions of the glass with different densities. Such regions have been postulated previously by several authors based on anomalous light scattering in the glass transition region [26–28]. Here we provide direct theoretical and experimental evidence in support of this notion for inorganic glass-forming systems. We also propose the nonmonotonic relaxation of density fluctuations as a means for characterizing this phenomenon.

Finally, we distinguish our work from the well-known ‘‘memory effect’’ [3] observed in glassy systems with nonexponential relaxation functions, often characterized in terms of a distribution of fictive temperatures. Depending on thermal history, the average fictive temperature of a glass can overshoot its equilibrium value during relaxation, leading to nonmonotonic decay of enthalpy, density, refractive index, etc. The nonmonotonic relaxation of density fluctuations reported here is not a result of the memory effect, since the glasses in this Letter are fully equilibrated at a single initial fictive temperature before undergoing isothermal relaxation at a new temperature. Hence, the fictive temperature relaxes monotonically, leading to monotonic decay of both enthalpy and density as in Figs. 1(a) and 2(a). However, during this monotonic decay of enthalpy and density, the fluctuations in those properties relax nonmonotonically due to dynamic inhomogeneities.

This work was supported in part by a grant from the National Science Foundation (NSF DMR 0603933) to S. S. The Advanced Light Source is supported by the U.S. DOE under Contract No. DE-AC03-76SF00098. We thank A. Hexemer, E. Schaible, and C. Wang for valuable technical assistance with SAXS data collection and A. Rovelstad for helpful discussions.

[1] P. K. Gupta and J. C. Mauro, J. Chem. Phys. **126**, 224504 (2007).
[2] J. C. Mauro, P. K. Gupta, and R. J. Loucks, J. Chem. Phys. **126**, 184511 (2007).
[3] G. W. Scherer, *Relaxation in Glass and Composites* (Krieger, Malabar, FL, 1992).
[4] F. H. Stillinger and T. A. Weber, Phys. Rev. A **25**, 978 (1982).
[5] F. H. Stillinger, J. Chem. Phys. **88**, 7818 (1988).
[6] F. H. Stillinger, J. Phys. Chem. B **102**, 2807 (1998).
[7] J. C. Mauro, R. J. Loucks, A. K. Varshneya, and P. K. Gupta, Sci. Model. Simul. **15**, 241 (2008).
[8] J. C. Mauro and R. J. Loucks, Phys. Rev. B **76**, 174202 (2007).
[9] A. N. Sreeram, A. K. Varshneya, and D. R. Swiler, J. Non-Cryst. Solids **128**, 294 (1991).
[10] R. Böhmer, K. L. Ngai, C. A. Angell, and D. J. Plazek, J. Chem. Phys. **99**, 4201 (1993).
[11] J. C. Mauro and R. J. Loucks, Phys. Rev. E **78**, 021502 (2008).
[12] J. C. Mauro, R. J. Loucks, J. Balakrishnan, and S. Raghavan, J. Chem. Phys. **126**, 194103 (2007).
[13] J. C. Mauro, R. J. Loucks, and P. K. Gupta, J. Phys. Chem. A **111**, 7957 (2007).
[14] Corning Glass Works, *Properties of Corning's Glass and Glass Ceramics Families* (Corning, New York, 1979).
[15] S. Sen, T. Topping, P. Yu, and R. E. Youngman, Phys. Rev. B **75**, 094203 (2007).
[16] J. H. Wendorff and E. W. Fischer, Kolloid Z. **251**, 876 (1973).
[17] V. Martinez, A. M. Jurdyc, D. Vouagner, C. Martinet, and B. Champagnon, J. Non-Cryst. Solids **351**, 2421 (2005).
[18] C. Levelut, R. Le Parc, A. Faivre, R. Bruning, B. Champagnon, V. Martinez, J.-P. Simon, F. Bley, and J.-L. Hazemann, J. Appl. Crystallogr. **40**, s512 (2007).
[19] J. Schroeder, M. A. Whitmore, M. R. Silvestri, S. K. Saha, and C. T. Moynihan, J. Non-Cryst. Solids **161**, 157 (1993).
[20] G. A. Appignanesi, J. A. Rodríguez Fris, and M. A. Frechero, Phys. Rev. Lett. **96**, 237803 (2006).
[21] B. V. R. Tata, P. S. Mohanty, and M. C. Valsakumar, Phys. Rev. Lett. **88**, 018302 (2001).
[22] A. Widmer-Cooper, P. Harrowell, and H. Fynewever, Phys. Rev. Lett. **93**, 135701 (2004).
[23] M. G. Mazza, N. Giovambattista, F. W. Starr, and H. E. Stanley, Phys. Rev. Lett. **96**, 057803 (2006).
[24] J. Qian, R. Hentschke, and A. Heuer, J. Chem. Phys. **111**, 10177 (1999).
[25] C. A. Angell, J. Non-Cryst. Solids **354**, 4703 (2008).
[26] R. E. Robertson, J. Polym. Sci., Polym. Phys. Ed. **17**, 597 (1979).
[27] E. Donth, J. Non-Cryst. Solids **53**, 325 (1982).
[28] C. T. Moynihan and J. Schroeder, J. Non-Cryst. Solids **160**, 52 (1993).